Supplementary Information (SI):

A synthetic *Escherichia coli* predator-prey system by Frederick K. Balagaddé et al

Contents

1. Model development

We model the dynamics of the synthetic *E. coli* predator-prey system (see Box 1) by accounting for the key reactions during the functioning of this system (Table S1, Figure S5). In writing down the kinetic rate expressions for these reactions, we make the following assumptions:

1) Cell growth follows logistic kinetics with a specific growth rate of k_{ci} (min^{-1}; i = 1 (predator) or 2 (prey); this convention is used throughout the text unless otherwise noted) and a carrying capacity of c_{max} for the predator and prey mixture. Numerical analysis shows that minimizing competition facilitates oscillatory behavior by preventing the total domination by one species. We further assume that the cell death rate is proportional to the concentration of the CcdB killer protein in the cell, with a rate constant of d_i (nM^{-1} min^{-1})
2) All components other than the cells are assumed to decay with first-order kinetics.
3) For constitutively expressed genes, the mRNA production rate is assumed to be constant. The synthesis rate of a protein is assumed to be proportional to the concentration of the corresponding mRNA.
4) The synthesis of AHLs occurs at a constant rate. This is equivalent to assuming that (a) the substrates for the synthesis reaction are in excess or sustained at a constant concentration and that (b) the corresponding AHL synthases (LuxI or RhlI) each have a constant intracellular concentration, which in turn can be achieved by expressing these enzymes constitutively.
5) The cognate transcriptional regulators (LuxR or RhlR) for AHLs are constitutively expressed.
6) Regulation of *ccdB* killer gene expression follows Michaelis-Menten-type kinetics. This is equivalent to assuming that (a) binding of a regulator to the promoter is fast and that (b) the rate of transcription is proportional to the concentration of active promoter – i.e., the concentration of the bound DNA if the promoter is to be activated, or that of the free DNA if the promoter is to be repressed. Note that synthesis of the killer mRNA is activated by the active RhlR in the prey, but repressed using an

engineered promoter(*1*) by the active LuxR in the predator. This assumption implies that there is no basal level of gene expression for un-induced or fully repressed promoters. We find that assuming a small basal level of gene expression in these cases will not change the overall dynamics.

7) Each AHL has uniform concentrations in a cell and in the well-mixed medium, and the only barrier for AHL transport is the cell membrane. The flux of AHL across the cell membrane is proportional to the concentration difference between the intracellular and extracellular space.
8) The binding of an AHL to its cognate regulator, the dissociation of the active regulator, and the dimerization of the active regulator follow mass action kinetics.
9) There is no crosstalk between different AHL signals.

The state variables and parameters are described in detail in Tables S2 and S3. Based on the listed reactions, we write a system of coupled ordinary differential equations (ODEs) to describe the interacting species.

Cell (predator-c_1, prey-c_2) growth and death

$$\frac{dc_1}{dt} = k_{c1}c_1\left(1 - \frac{c_1 + c_2}{c_{\max}}\right) - \frac{d_1E_1c_1}{1 + \alpha_A A} - Dc_1 \tag{S1}$$

$$\frac{dc_2}{dt} = k_{c2}c_2\left(1 - \frac{c_1 + c_2}{c_{\max}}\right) - d_2E_2c_2 - Dc_2 \tag{S2}$$

Expression of regulator genes (luxR for predator; lasR for prey, denoted by M_{Ri}) and decay of products (R_i)

$$\frac{dM_{Ri}}{dt} = v_{MRi} - d_{MRi}M_{Ri} \tag{S3}$$

$$\frac{dR_i}{dt} = k_{Ri}M_{Ri} - d_{Ri}R_i - k_{Pi}A_{aj}R_i + d_{Pi}P_i \tag{S4}$$

Activation of regulator-inducer complex (R_1-A_{a2} = P_1, and R_2-A_{a1} = P_2)

$$\frac{dP_i}{dt} = k_{Pi} A_{aj} R_i - d_{Pi} P_i \tag{S5}$$

Expression of antidote gene (ccdA, denoted by M_A here) and protein (A) in predator

$$\frac{dM_A}{dt} = \frac{k_{MA} \alpha_{MA} P_1^{\beta}}{1 + \alpha_{MA} P_1^{\beta}} - d_{MA} M_A \tag{S6}$$

$$\frac{dA}{dt} = k_A M_A - d_A A \tag{S7}$$

Expression of killer genes (M_{E1}, M_{E2}) and decay of products (E_1, E_2)

$$\frac{dM_{E1}}{dt} = \alpha_{ME1} - d_{ME1} M_{E1} \tag{S8}$$

$$\frac{dM_{E2}}{dt} = \frac{k_{ME2} \alpha_{ME2} P_2^{\beta}}{1 + \alpha_{ME2} P_2^{\beta}} - d_{ME2} M_{E2} \tag{S9}$$

$$\frac{dE_i}{dt} = k_{Ei} M_{Ei} - d_{Ei} E_i \tag{S10}$$

Where β (approximately 1.2) represents the cooperation Hill coefficient of gene expression.

Product, diffusion and decay of AHLs (A_1: 3OC12HSL from predator; A_2: 3OC6HSL from prey)

$$\frac{dA_i}{dt} = v_{Ai} - \eta_i (A_i - A_{ei}) - d_{Ai} A_i \tag{S11}$$

$$\frac{dA_{ei}}{dt} = \eta_i \frac{c_i}{1 - c_1 - c_2} (A_i - A_{ei}) - \eta_i \frac{c_j}{1 - c_1 - c_2} (A_{ei} - A_{ai}) - d_{Aei} A_{ei} - DA_{ei} \tag{S12}$$

$$\frac{dA_{ai}}{dt} = \eta_i (A_{ei} - A_{ai}) - d_{Aai} A_{ai} - k_{Pj} A_{ai} R_j + d_{Pj} P_j \tag{S13}$$

These equations highlight the overall symmetric structure of the model: the same form of kinetics is followed by the corresponding components in the two cell types, except for the transcription of killer genes, which are regulated differently in the two cell types. In equation S12, the rate of AHL diffusion must be scaled for the extracellular AHL concentrations by the ratio of the intracellular volume to the extracellular volume, since the AHLs will be diluted in

the extracellular space. In the same equation, the index j represents the source cell for the production of AHLi.

Simplification of the model

To simplify the model, we assume that several components are at a quasi-steady state. These components include all mRNAs, transcriptional regulators, killer proteins. This is equivalent to assuming that processes leading to changes in these species are at a much faster time scale than the rest of the processes. We find that these simplifying assumptions will not significantly change the qualitative nature of the system dynamics.

By solving for the steady state levels of these variables and substituting them into the remaining equations, we reduce the full model into 4 ODEs: two equations describing the cell populations, two describing the levels of the AHLs in the medium. The major difference occurs in the equations describing the different effects of the two AHLs in the death of predator and prey cells.

$$\frac{dc_1}{dt} = k_{c1}c_1\left(1 - \frac{c_1 + c_2}{c_{\max}}\right) - d_{c1}c_1\frac{K_1}{K_1 + A_{e2}^{\beta}} - Dc_1 \tag{S14}$$

$$\frac{dc_2}{dt} = k_{c2}c_2\left(1 - \frac{c_1 + c_2}{c_{\max}}\right) - d_{c2}c_2\frac{A_{e1}^{\beta}}{K_2 + A_{e1}^{\beta}} - Dc_2 \tag{S15}$$

$$\frac{dA_{e1}}{dt} = k_{A1}c_1 - (d_{Ae1} + D)A_{e1} \tag{S16}$$

$$\frac{dA_{e2}}{dt} = k_{A2}c_2 - (d_{Ae2} + D)A_{e2} \tag{S17}$$

where c_1 is the predator population (per 10^3 cells μl^{-1}), c_2 the prey population, A_{e1} the 3OC12HSL concentration (nM), and A_{e2} the 3OC6HSL concentration (nM). The parameters are defined as following; $K_1 = \frac{1}{\left(\alpha_A \frac{k_A}{d_A}\frac{k_{MA}}{d_{MA}} + 1\right)\alpha_{MA}\left(\frac{k_{p1}}{d_{p1}}\frac{k_{R1}}{d_{R1}}\frac{v_{MR1}}{d_{MR1}}\right)^{\beta}}$, $K_2 = \frac{1}{\alpha_{ME2}a_2^{\beta}}$, $d_{c1} = d_1\frac{k_{E1}}{d_{E1}}\frac{\alpha_{ME1}}{d_{ME1}}$, $d_{c2} = d_2\frac{k_{E2}}{d_{E2}}\frac{k_{ME2}}{d_{ME2}}$. These parameters lump effects of regulator synthesis,

binding of AHL to its cognate regulator, and dimerization of the active regulator. β =2 in the Hill functions of equations (S14-S15) indicate the dimerization of the active regulators, which leads to a cooperativity for the regulation of killer gene synthesis. This value results from the dimerization of active regulators. However, the actual cooperativity is usually smaller than 2 (Cynthia Collins (unpublished data), also see reference(*2*)).

From these equations, the basic logic of the circuit is evident: an increase in c_2 (the prey density) will result in a decrease in A_{e2}, thus a reduced death rate for c_1 (the predator density). The increase in c_1, however, will lead to an increase in A_{e1}, which in turn will lead to a larger death rate for the prey. The bifurcation analyses were performed using XPPAUT (http://www.math.pitt.edu/~bard/xpp/xpp.html).

It is worth noting that further reduction of the model, for example by assuming the autoinducers (AHLs) to be at a quasi-steady state, drastically changes the qualitative behavior of the system (results not shown). In particular, the over-simplified system fails to oscillate for all parameter settings. This additional analysis indicates that gene regulation needs to be at a similar time scale as the population dynamics in order to generate stable oscillations. It also highlights a key difference between this system and conventional two-species predator-prey systems, where two equations are sufficient to generate oscillations(*3*).

Parameter values

The base parameter setting of the model is listed in Table S4. Several parameter values are directly taken from the literature or derived from literature data. For other parameters where we lack quantitative information (for example, those governing gene expression process), we use educated guesses that are biologically feasible and able to simulate our experimental findings.

In the circuit diagram (Figure S5), the $p_{lac\text{-}ara\text{-}1}$ promoter is activated upon exposure to IPTG. Subsequently, the predator killing rate (d_{c1}) is increased by increased ccdB expression, and the 3OC6HSL synthesis rate (k_{A2}) by prey is increased. To model the impact of IPTG on

the circuit activation, we introduce the following functional expressions:

$$d_{c1} = 0.5 + 1 \times \frac{[\mathrm{IPTG}]^2}{5^2 + [\mathrm{IPTG}]^2} \tag{S18}$$

$$k_{A2} = 0.02 + 0.03 \times \frac{[\mathrm{IPTG}]^2}{5^2 + [\mathrm{IPTG}]^2} \tag{S19}$$

Stochastic differential equations (SDEs):

In order to account for the effect of the stochastic but small variance in experimental setup, we employed the following SDEs (adding a noise term in Eqs. S14-17):

$$\frac{dc_1}{dt} = k_{c1}c_1\left(1 - \frac{c_1 + c_2}{c_{\max}}\right) - d_{c1}c_1\frac{K_1}{K_1 + A_{e2}^{\beta}} - Dc_1 + \varepsilon \cdot \xi \tag{S20}$$

$$\frac{dc_2}{dt} = k_{c2}c_2\left(1 - \frac{c_1 + c_2}{c_{\max}}\right) - d_{c2}c_2\frac{A_{e1}^{\beta}}{K_2 + A_{e1}^{\beta}} - Dc_2 + \varepsilon \cdot \xi \tag{S21}$$

$$\frac{dA_{e1}}{dt} = k_{A1}c_1 - (d_{Ae1} + D)A_{e1} + \varepsilon \cdot \xi \tag{S22}$$

$$\frac{dA_{e2}}{dt} = k_{A2}c_2 - (d_{Ae2} + D)A_{e2} + \varepsilon \cdot \xi \tag{S23}$$

where ξ is the noise term that satisfies normal distribution with zero mean and unit variance, and ε is the noise amplitude. XPPAUT software is used to simulate the SDEs using Euler method.

Table S1. Reactions described in the full model (1=predator and 2 = prey; the same form of kinetics is assumed for both the predator and the prey unless noted otherwise)

Reaction	Rate	Description
Population dynamics		
$\rightarrow c_i$ [a]	$k_i(c_{\max i} - c_i)/c_{\max i}$	Cell growth
$c_i \rightarrow$	$d_i E_i c_i$	Cell death
Expression of killer genes and decay of products		
$\rightarrow E_i$	$k_{Ei} M_{Ei}$	CcdB killer protein production
$E_i \rightarrow$	$d_{Ei} E_i$	killer protein decay
$\rightarrow M_{E1}$	$\frac{k_{ME1}}{1+\alpha_{ME1} Q_1}$	Transcription of killer gene in the predator
$\rightarrow M_{E2}$	$\frac{k_{ME2}\alpha_{ME2} Q_2}{1+\alpha_{ME2} Q_2}$	Transcription of killer gene in the prey
$M_{Ei} \rightarrow$	$d_{MEi} M_{Ei}$	killer mRNA decay
Production, diffusion, and decay of AHLs		
$\rightarrow A_i$ [b]	ν_{Ai}	Synthesis of AHL
$A_i \rightarrow$	$d_{Ai} A_{ai}$	Decay of AHL in its source cell
$A_i \rightarrow A_{ei}$	$\eta_i (A_i - A_{ei})$	Diffusion of AHL from its source cell
$A_{ei} \rightarrow$	$d_{Aei} A_{ei}$	Decay of AHL in the medium
$A_{ei} \rightarrow A_{ai}$	$\eta_i (A_{ei} - A_{ai})$	Diffusion of AHL to its target cell
$A_{ai} \rightarrow$	$d_{Ai} A_i$	Decay of AHL in its target cell
Production and decay of transcriptional regulators		
$\rightarrow R_i$	$k_{Ri} M_{Ri}$	Production of regulator
$R_i \rightarrow$	$d_{Ri} R_i$	Decay of regulator
$\rightarrow M_{Ri}$	ν_{MRi}	Production of regulator mRNA
$M_{Ri} \rightarrow$	$d_{MRi} M_{Ri}$	Decay of regulator mRNA
Activation of transcriptional regulators by AHLs		
$R_i + A_{ai} \rightarrow P_i$	$k_{Pi} A_{ai} R_i$	Binding of AHL to its cognate regulator
$P_i \rightarrow R_i + A_{ai}$	$d_{Pi} P_i$	Dissociation of AHL-regulator complex
$2P_i \rightarrow Q_i$	$k_{Qi} P_i^2$	Dimerization of AHL-regulator complex
$Q_i \rightarrow 2P_i$	$d_{Qi} Q_i$	Dissociation of AHL-regulator complex dimer

[a] Reactants for this reaction are not specified. Similarly, when the right-hand-side of a reaction is empty (for example for all the decay reactions), products of the reaction are not specified.

[b] AHLs are indexed based on the their target cells: AHL1 is produced in the prey while AHL2 is produced in the predator.

Table S2. State variables of the full model

Variable	Description
c_i	Cell density [a]
E_i	[CcdB killer protein] [b]
M_{Ei}	[killer-mRNA]
A_i	[AHL] in the source cell
A_{ei}	[AHL] in the medium
A_{ai}	[AHL] in the target cell
R_i	[regulator]
M_{Ri}	[regulator mRNA]
P_i	[AHL-regulator complex]
Q_i	[(AHL-regulator complex)$_2$]

[a] Cell density is measured as number of cells per ml^{-1}.

[b] The notation [X] represents the concentration of component X.

Table S3. Kinetic parameters of the full model

Parameter	Description	Unit
k_i	Specific cell growth rate constant	min^{-1}
$c_{\max i}$	Carrying capacity for cell growth	ml^{-1}
d_i	Cell death rate constant	$nM^{-1}min^{-1}$
k_{Ei}	CcdB killer protein synthesis rate constant	min^{-1}
d_{Ei}	CcdB killer protein decay rate constant	min^{-1}
k_{MEi}	Maximal rate of *ccdB* killer gene transciption	$nM\ min^{-1}$
α_{MEi}	Sensitivity of *ccdB* killer gene transcription to AHL	nM^{-1}
d_{MEi}	killer mRNA decay rate constant	min^{-1}
ν_{MRi}	Transcription rate for a regulator	$nM\ min^{-1}$
d_{MRi}	Regulator mRNA decay rate constant	min^{-1}
k_{Ri}	Regulator synthesis rate constant	min^{-1}
d_{Ri}	Regulator decay rate constant	min^{-1}
ν_{Ai}	AHL synthesis rate constant	$nM\ min^{-1}$
η_i	AHL diffusion rate constant across the cell membrane	min^{-1}
d_{Ai}	AHL intracellular decay rate constant	min^{-1}
d_{Aei}	AHL extracellular decay rate constant	min^{-1}
k_{Pi}	AHL/regulator binding rate constant	$nM^{-1}min^{-1}$
d_{Pi}	AHL/regulator dissociation rate constant	min^{-1}
k_{Qi}	AHL-regulator complex dimerization rate constant	$nM^{-1}min^{-1}$
d_{Qi}	$(AHL\text{-}regulator)_2$ unbinding rate constant	min^{-1}

Table S4. Base values for the key parameters in Equations S14-S19 (*4-6*)

Parameter	Description	Base value
k_{c1}	Predator cell (MG1655) growth rate constant	0.8 hr^{1}
k_{c2}	Prey cell (Top10F') growth rate constant	0.4 hr^{1}
c_{max}	Carrying capacity for cell growth	100 $\times 10^{3}$ cells nL^{-1}
β	Cooperativity of AHL effect	2
d_{c2}	Prey cell death rate constant	0.3 hr^{-1}
K_i	Concentration of AHL necessary to half-maximally active PluxI promoter	10 nM
k_{A1}	Synthesis rate constant of AHL by the predator cell	0.1 nM ml hr^{-1}
d_{Ae1}	Decay rate constant of 3OC12HSL in the cell (*6*)	0.017 hr^{1}
d_{Ae2}	Decay rate constant of 3OC6HSL in the cell (*6*)	0.11 hr^{1}
D	Dilution rate	0 - 0.3 hr^{-1}

"*D*" (hr^{-1}) is a dilution rate and calculated with the relation $D = -\frac{\ln[1-F]}{T}$ where *F* is a fraction of dilution and *T* the time interval between each dilution event: for example, D = 0.2 hr^{-1} for 25% discrete dilution (*F* = 1/4) every 1 hours (*T*) (*4*).

References

1. K. A. Egland, E. P. Greenberg, *J Bacteriol* 182, 805 (Feb, 2000).
2. J. Zhu, S. C. Winans, *Proc Natl Acad Sci U S A* 96, 4832 (1999).
3. R. M. May, *Stability and complexity in model ecosystems* (Princeton University Press, Princeton, NJ, USA, ed. 2, 1974), pp. 265.
4. F. K. Balagadde, L. C. You, C. L. Hansen, F. H. Arnold, S. R. Quake, *Science* 309, 137 (Jul, 2005).
5. L. You, R. S. Cox, 3rd, R. Weiss, F. H. Arnold, *Nature* 428, 868 (2004).
6. G. F. Kaufmann *et al.*, *Proceedings Of The National Academy Of Sciences Of The United States Of America* 102, 309 (Jan 11, 2005).

2. Supplementary figure legends and figures

Figure S1. Microchemostat design illustrating modifications that allow for accurate monitoring of community composition. **(A)** New microchemostat reactor design with circular growth chamber loop. The imaging section has been enlarged to show the ~3 μm high strips incorporated along the growth loop track (compared to a ~10 μm height otherwise). **(B)** Three dimensional schematic of the imaging section along the growth loop. **(C)** Sample fluorescent image, showing well-resolved fluorescent bacteria in the ~3 μm tall imaging section (center), compared to the unresolved signal in the ~10 μm tall sections at the edges. The imaged cells are constrained to a thin vertical height to put them all in focus simultaneously.

Figure S2. Killing dynamics by LacZα-CcdB and LacZα'-CcdB. In plasmids placCcdB (LacZα-CcdB, p15A origin, Kan^R) and placCcdBs (LacZα'-CcdB, p15A origin, Kan^R), the killer gene is under the control of $P_{lac/ara-1}$ promoter. Each was introduced into Top10F' (Invitrogen) cells. Full-grown cultures were incubated in 2 ml of LB media with 1mM IPTG at 37˚C and 250 r.p.m. in 12 ml test tubes. Colony forming units (CFU) were measured after IPTG induction at different time points as indicated.

Figure S3. Test of communication and crosstalk between LuxI/LuxR and LasI/LasR systems in Top10F' predator and prey cells on agar plate. Receiver cells were spread on agar plates with IPTG, which induced expression of the transcription regulators (LuxR or LasR). Receiver cells will express a killer protein (*LacZα-ccdB*) when sensing appropriate signals. Receiver 1, which encodes LuxR, responded to cells (Top10F' cells containing pLuxRI) sending 3OC6HSL (as indicated by the death zone around the sender cells) but did not respond to cells (Top10F' cells containing pLasRI) sending 3OC12HSL. Receiver 2, which encodes LasR, responded to cells sending 3OC12HSL but not cells sending 3OC6HSL.

Figure S4. Configurations of the plasmids in two pairs of predator and prey. Each strain carries two plasmids. The bracket after the plasmid name indicates (replication origin, selection marker gene). *LacZα'-ccdB* is derived from *lacZα-ccdB* by deleting 96 in frame base pairs (see Methods). **(A)** The pair of predator (MG1655) and prey (Top10F'). **(B)** A different

pair of predator (Top10F') and prey (Top10F').

Figure S5. The detailed reaction mechanism in the predator-prey ecosystem, which was schematically depicted in Box 1.

Figure S6. Long-term characterization of predator-prey dynamics for varying induction levels by IPTG in a single microchemostat experiment (other experiments implemented simultaneously with experiments in Figure 2B). The predator was implemented in MG1655 cell strain and the prey was in Top10F' (Figure S4A). The microchemostat dilution rate was: 0.1125 hr^{-1}. Without induction of the circuit by IPTG: prey cells are washed out of microchemostat, and only predator cells exist. At increased IPTG level (IPTG = 5 μM or above), oscillatory dynamics of predator and prey populations may be elicited.

Figure S7. Parallel experiments in different microchemostat reactors generated simultaneously with Figure 3A & B show the impact of the dilution rate (D) on the systems dynamics. **(A)** Other experiments generated simultaneously with Figure 3A. Experimental dynamics of predator and prey populations at different IPTG concentrations and different D in microchemostat: for the pair of predator (MG1655) and prey (Top10F'). Before 223 hours, D= 0.11 hr^{-1} and after, D = 0.20 hr^{-1} as demarcated on the graphs. Changing D may change the system dynamics from long period of oscillation (only a partial cycle is shown here) to damped oscillation. The data also show that the transient damped oscillatory dynamics is rather sensitive to variation of operating parameters (e.g., see Row 3, IPTG=50 μM). **(B)** Other experiments generated simultaneously with Figure 3B (For the pair of predator (Top10F') and prey (Top10F')). In all reactors except row 2, columns 1&2, the predator was washed out at the beginning of the experiment. [IPTG] = 50 μM; D = 0.15 hr^{-1} for (0-155 hrs), D=0.23 hr^{-1} for (155-245 hrs), D= 0.3 hr^{-1} beyond 245 hrs. **(C)** Two-parameter bifurcation diagram (by analyzing Equations S14-S19) in the parameter plane of ([IPTG], D). The parameter region bounded by the loci of Hopf bifurcation points is where oscillatory dynamics occurs (see insets). At the parameter regime that is beyond but close to the loci of Hopf bifurcation points, the system demonstrates damped oscillation. Damped oscillations are transient dynamics which is fairly sensitive to the small perturbation of parameters or initial

phases of predator and prey population (see insets). The periods of oscillations decreases upon increasing dilution rate D.

Figure S8. Stochastic effects drastically impact on the system dynamics demonstrated by the numerical simulation of the SDEs (Eqs. S20-S23). (A) The period of the oscillations may be significantly changed by noise. Two representative set of simulation results with different random number sets are shown. (B) At some random number sets, the predator may extinct after some time (two representative time courses are illustrated). In such situation, sustained oscillation is damaged by stochastic noise. In all these simulation results, the same parameter setting and the same initial conditions are used. Each time course corresponds to a different random number set, respectively. The noise amplitude in the equations is $\varepsilon = 0.1$. XPPAUT is employed to numerically simulate the SDEs with Euler method. The corresponding ODEs simulation result was shown in Fig. 2C (time course with [IPTG] = 1000 μM).

Figure S1:

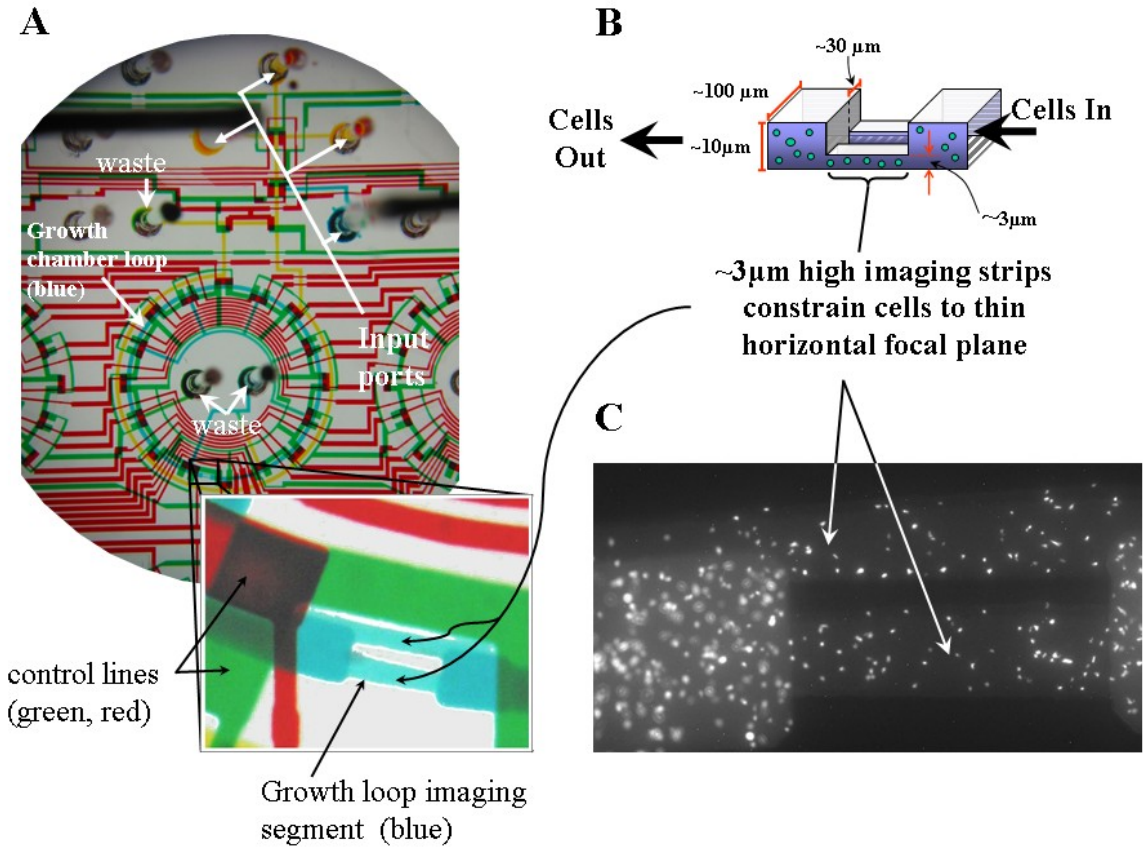
A
waste
Growth chamber loop (blue)
Input ports
waste
control lines (green, red)
Growth loop imaging segment (blue)
B
~30 µm
~100 µm
Cells Out
~10µm
Cells In
~3µm
~3µm high imaging strips constrain cells to thin horizontal focal plane
C

Figure S2:

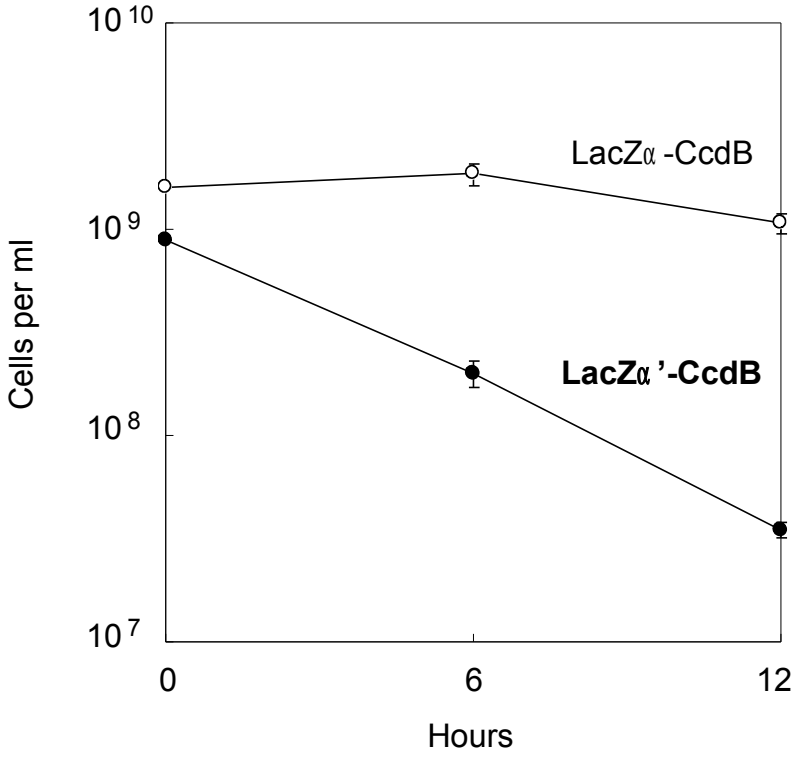
10 10
10 9
10 8
10 7
Cells per ml
LacZα -CcdB
LacZα '-CcdB
0
6
12
Hours

Figure S3:

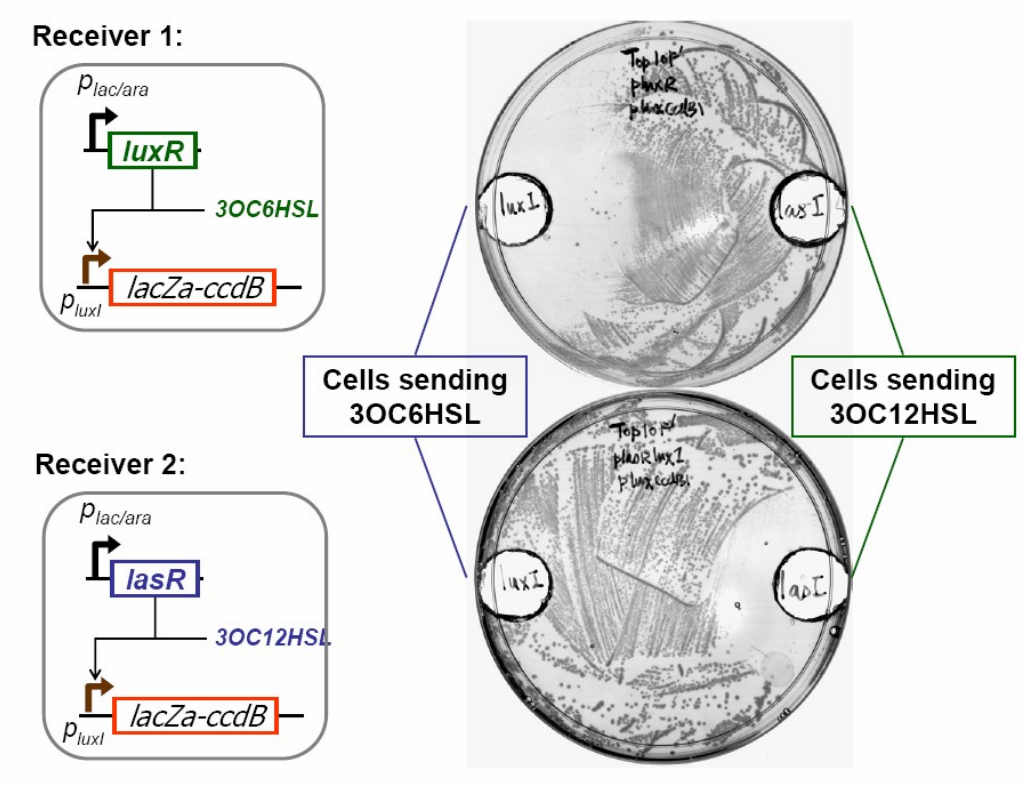
Receiver 1:
$p_{lac/ara}$
luxR
3OC6HSL
p_{luxI}
lacZa-ccdB
Receiver 2:
$p_{lac/ara}$
lasR
3OC12HSL
p_{luxI}
lacZa-ccdB
luxI
lasI
Cells sending 3OC6HSL
Cells sending 3OC12HSL

Figure S4:

A.

Predator (MG1655)

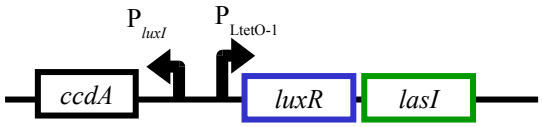

ptetLuxRLasI-*lux*CcdA (SC101, Cm^R)

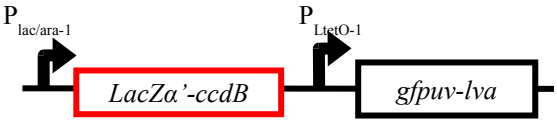

placCcdBs-gfpuv(lva) (p15A, Kan^R)

Prey (Top10F')

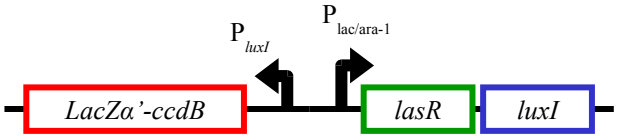

pLasRLuxI-*lux*CcdBs (p15A, Kan^R)

B.

Predator (Top10F')

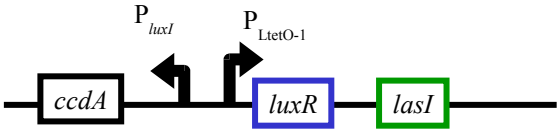

ptetLuxRLasI-*lux*CcdA (SC101, Cm^R)

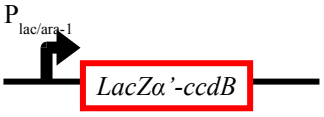

placCcdBs (p15A, Kan^R)

Prey (Top10F')

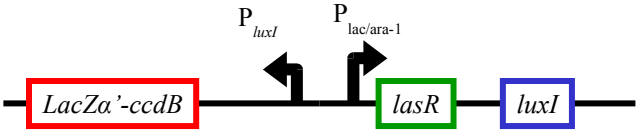

pLasRLuxI-*lux*CcdBs (p15A, Kan^R)

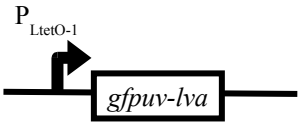

ptetGFPuv(LVA) (ColE1, Cm^R)

Figure S5:

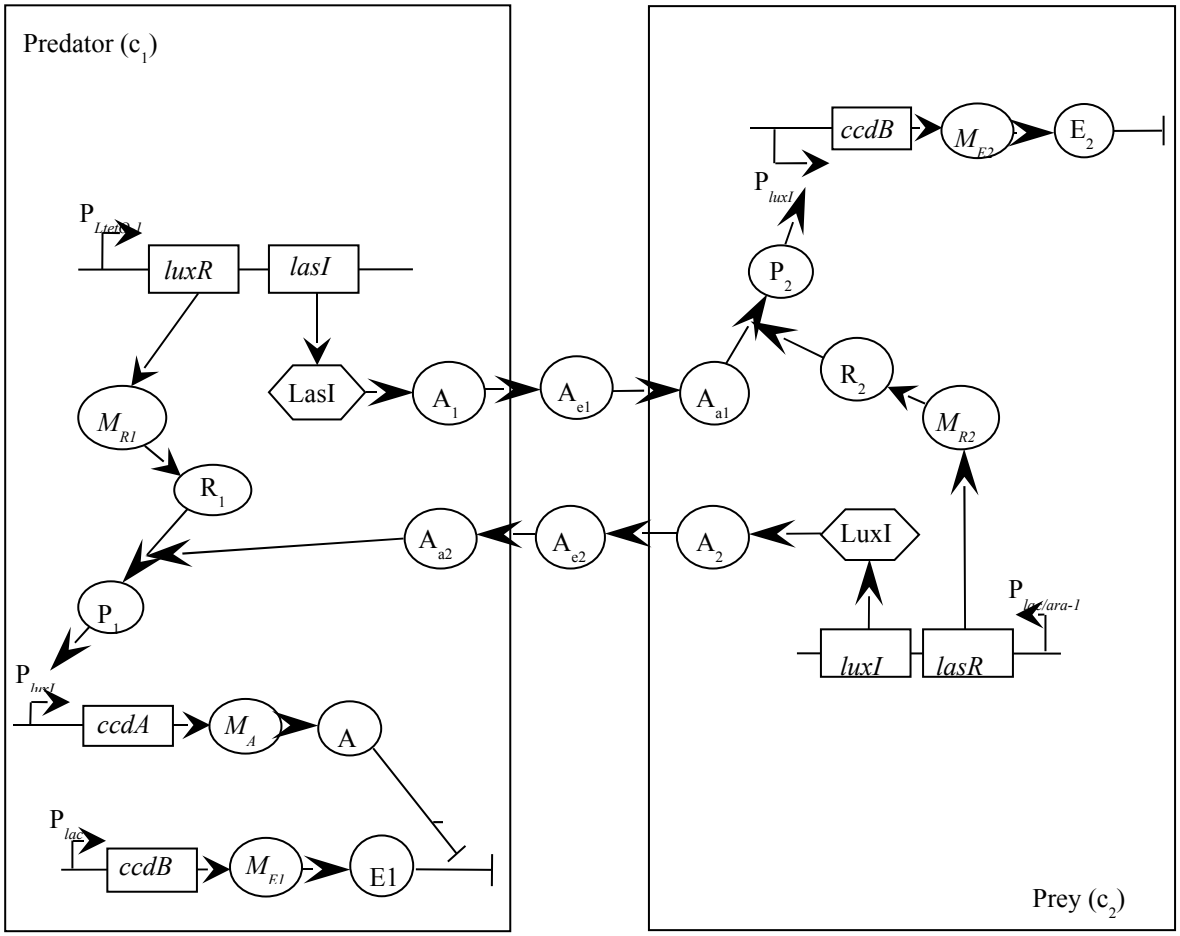
Predator (c_1)
$P_{Lux/lac-1}$
luxR
lasI
LasI
A_1
A_{e1}
M_{R1}
R_1
P_1
A_{a2}
A_{e2}
P_{luxI}
ccdA
M_A
A
P_{lac}
ccdB
M_{E1}
E1
ccdB
M_{E2}
E_2
P_{luxI}
P_2
R_2
M_{R2}
A_{a1}
A_2
LuxI
$P_{lac/ara-1}$
luxI
lasR
Prey (c_2)

Figure S6

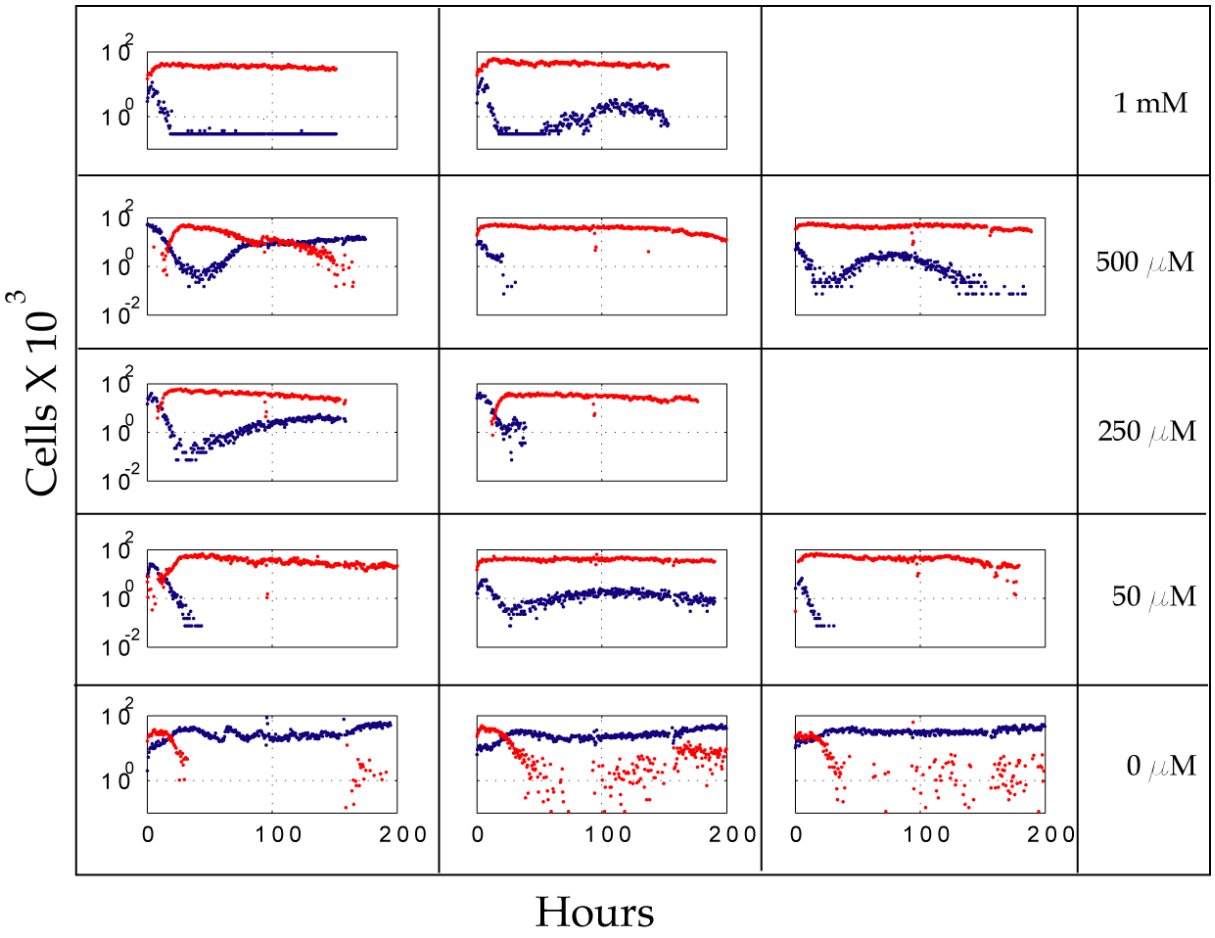
Cells X 10^3
Hours
1 mM
500 μM
250 μM
50 μM
0 μM
10^2
10^0
10^-2
0
100
200

Figure S7A

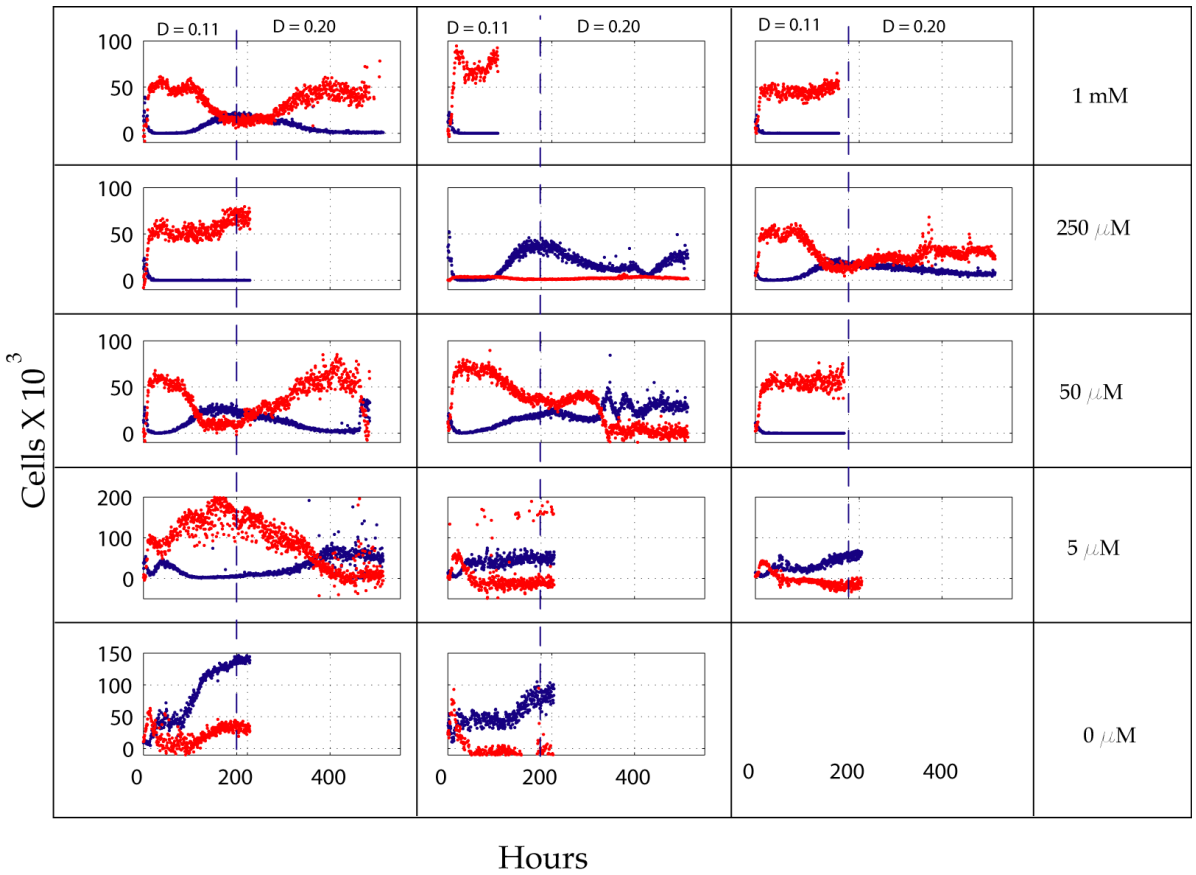

Figure S7B

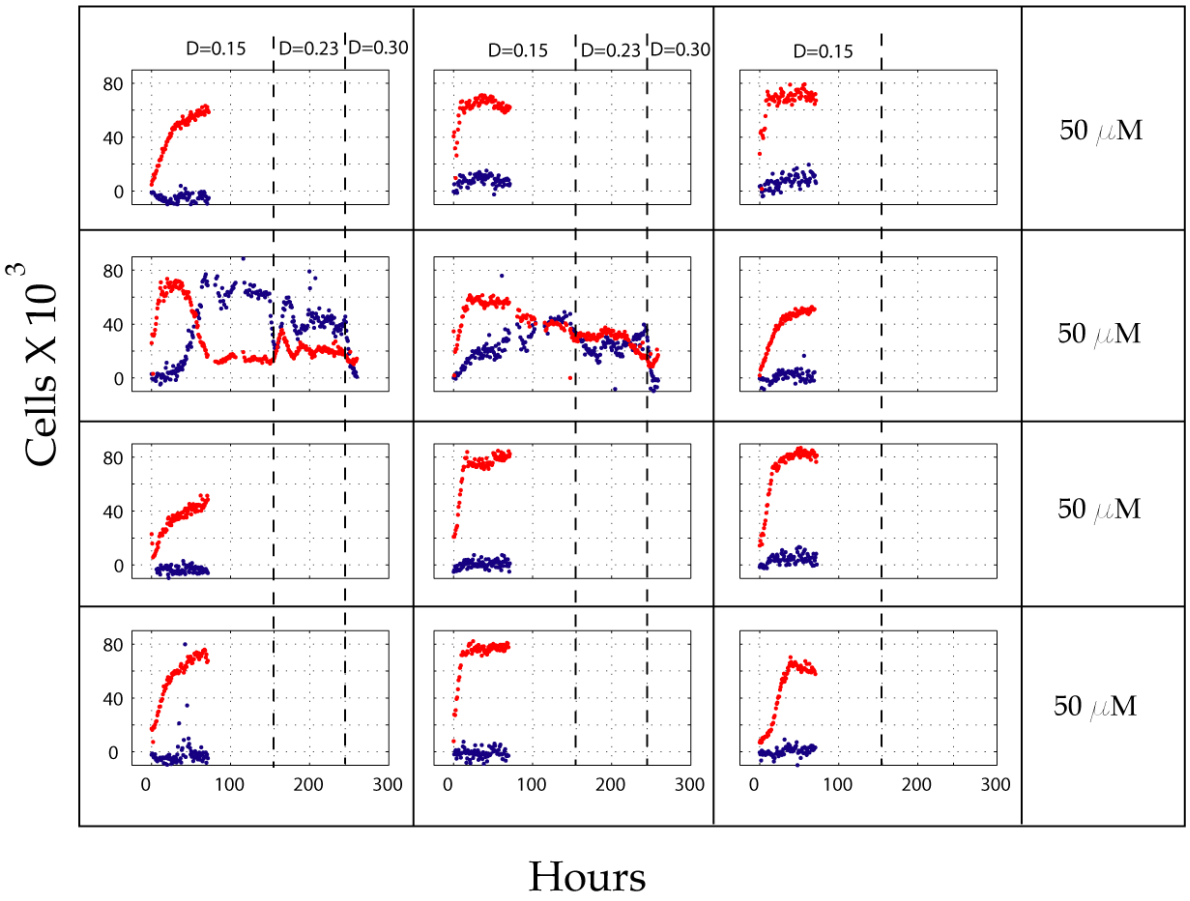
D=0.15
D=0.23
D=0.30
D=0.15
D=0.23
D=0.30
D=0.15
80
40
0
0
100
200
300
50 μM
50 μM
50 μM
50 μM
Cells X 10^3
Hours

Figure S7C

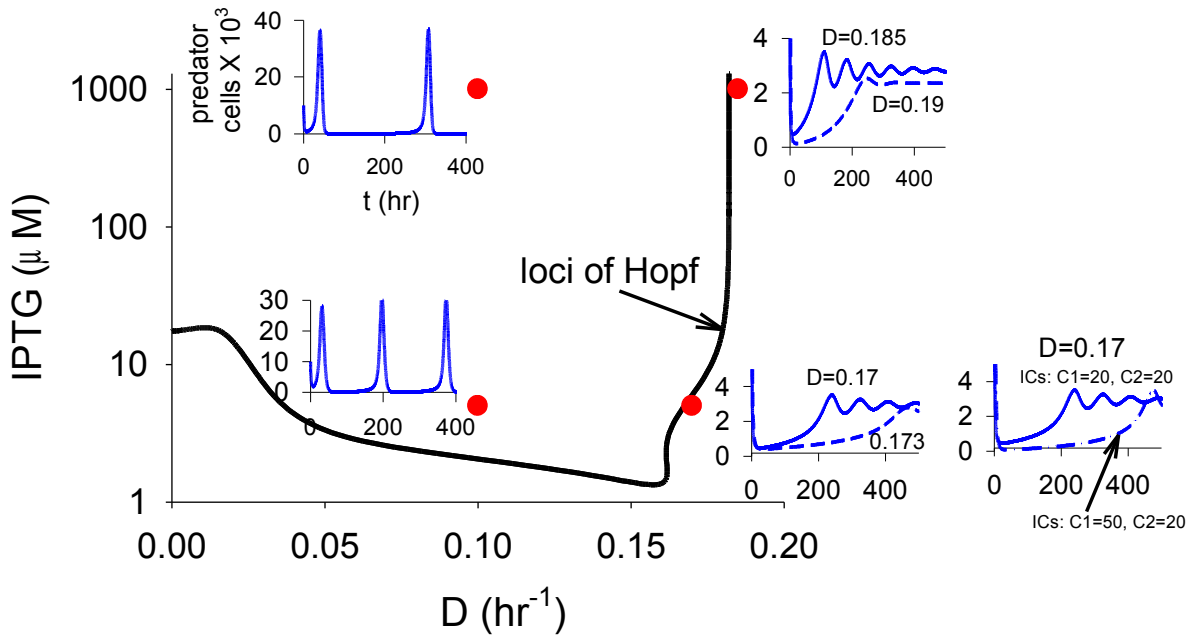
predator cells X 10^3
t (hr)
IPTG (μ M)
D (hr^-1)
loci of Hopf
D=0.185
D=0.19
D=0.17
0.173
D=0.17
ICs: C1=20, C2=20
ICs: C1=50, C2=20

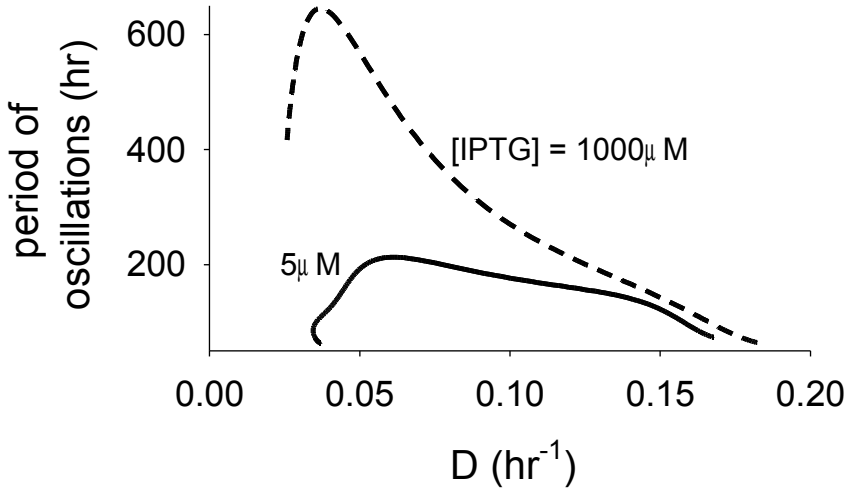
period of oscillations (hr)
[IPTG] = 1000μ M
5μ M
D (hr^-1)

Figure S8.